Order and magnetic structures

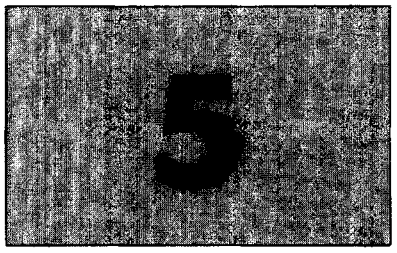

In the previous chapter the different types of magnetic interaction which operate between magnetic moments in a solid have been presented. In this chapter we will consider the different types of magnetic ground state which can be produced by these interactions. Some of these ground states are illustrated in Fig. 5.1. The different ground states include ferromagnets in which all the magnetic moments are in parallel alignment, antiferromagnets in which adjacent magnetic moments lie in antiparallel alignment, spiral and helical structures in which the direction of the magnetic moment precesses around a cone or a circle as one moves from one site to the next, and spin glasses in which the magnetic moments lie in frozen random arrangements. This chapter will be concerned with showing how, in broad terms, the interactions discussed in the previous chapter lead to these differing ground states. In the following chapter the phenomenon of order will be examined in a more general context and it will be seen that order is a consequence of broken symmetry.

Notation reminder: In this book J refers to the exchange constant, J is total angular momentum.

5.1 Ferromagnetism

A ferromagnet has a spontaneous magnetization even in the absence of an applied field. All the magnetic moments lie along a single unique direction.[1] This effect is generally due to exchange interactions which were described in the previous chapter. For a ferromagnet in an applied magnetic field $\mathbf{B}$, the appropriate Hamiltonian to solve is

$$\hat{\mathcal{H}} = -\sum_{ij} \mathsf{J}_{ij} \mathbf{S}_i \cdot \mathbf{S}_j + g\mu_B \sum_j \mathbf{S}_j \cdot \mathbf{B}, \tag{5.1}$$

and the exchange constants for nearest neighbours will be positive in this case, to ensure ferromagnetic alignment. The first term on the right is the Heisenberg exchange energy (see eqn 4.7). The second term on the right is the Zeeman energy (see eqn 1.35). To keep things simple to begin with, let us assume[2] that we are dealing with a system in which there is no orbital angular momentum, so that $L = 0$ and $J = S$.

[1] In fact in many ferromagnetic samples this is not true throughout the sample because of domains. In each domain there is a uniform magnetization, but the magnetization of each domain points in a different direction from its neighbours. See Section 6.7 for more on magnetic domains.

[2] We will relax this assumption later in Section 5.1.4.

5.1.1 The Weiss model of a ferromagnet

To make progress with solving eqn 5.1 it is necessary to make an approximation. We define an effective molecular field at the i^{th} site by

$$\mathbf{B}_{\text{mf}} = -\frac{2}{g\mu_B} \sum_j \mathsf{J}_{ij} \mathbf{S}_j. \tag{5.2}$$

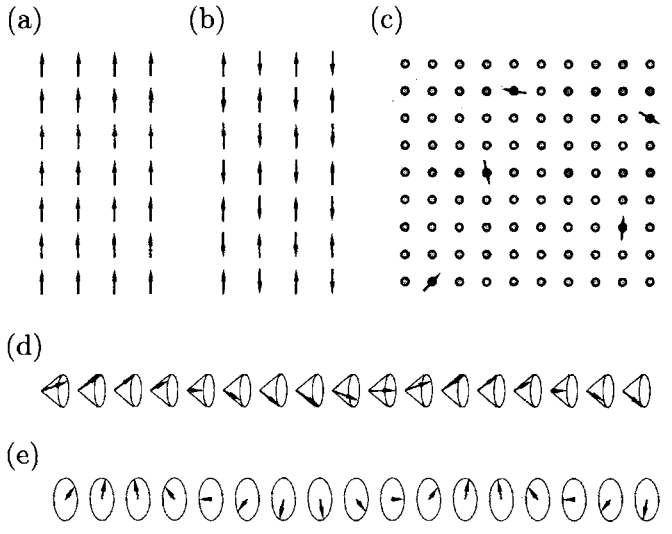

Fig. 5.1 Various spin arrangements in ordered systems: (a) ferromagnets, (b) antiferromagnets, (c) spin glasses and (d) spiral and (e) helical structures.

Now focus on the i^{th} spin. Its energy is due to a Zeeman part $g\mu_B \mathbf{S}_i \cdot \mathbf{B}$ and an exchange part. The total exchange interaction between the i^{th} spin and its neighbours is $-2\sum_j \mathsf{J}_{ij}\mathbf{S}_i \cdot \mathbf{S}_j$, where the factor of 2 is because of the double counting.[3] This term can be written as

[3] See Section 4.2.1.

$$-2\mathbf{S}_i \cdot \sum_j \mathsf{J}_{ij}\mathbf{S}_j = -g\mu_B \mathbf{S}_i \cdot \mathbf{B}_{\text{mf}}. \tag{5.3}$$

Hence the exchange interaction is replaced by an effective molecular field $\mathbf{B}_{\text{mf}}$ produced by the neighbouring spins. The effective Hamiltonian can now be written as

$$\hat{\mathcal{H}} = g\mu_B \sum_i \mathbf{S}_i \cdot (\mathbf{B} + \mathbf{B}_{\text{mf}}) \tag{5.4}$$

which now looks like the Hamiltonian for a paramagnet in a magnetic field $\mathbf{B} + \mathbf{B}_{\text{mf}}$. The assumption underpinning this approach is that all magnetic ions experience the same molecular field. This may be rather questionable, particularly at temperatures close to a magnetic phase transition, as will be discussed in the following chapter. For a ferromagnet the molecular field will act so as to align neighbouring magnetic moments. This is because the dominant exchange interactions are positive. (For an antiferromagnet, they will be negative.)

Since the molecular field measures the effect of the ordering of the system, one can assume that

$$\mathbf{B}_{\text{mf}} = \lambda \mathbf{M} \tag{5.5}$$

where λ is a constant which parametrizes the strength of the molecular field as a function of the magnetization. For a ferromagnet, $\lambda > 0$. Because of the large Coulomb energy involved in the exchange interaction, the molecular field is often found to be extremely large in ferromagnets.

We are now able to treat this problem as if the system were a simple paramagnet placed in a magnetic field $\mathbf{B} + \mathbf{B}_{\text{mf}}$. At low temperature, the moments can be aligned by the internal molecular field, even without any applied field

being present. Notice that the alignment of these magnetic moments gives rise to the internal molecular field that causes the alignment in the first place, so that this is something of a 'chicken-and-egg' scenario. At low temperature the magnetic order is self-sustaining. As the temperature is raised, thermal fluctuations begin to progressively destroy the magnetization and at a critical temperature the order will be destroyed. This model is known as the **Weiss model of ferromagnetism**.

Pierre Weiss (1865–1946)

To find solutions to this model, it is necessary to solve simultaneously the equations

$$\frac{M}{M_s} = \mathrm{B}_J(y) \tag{5.6}$$

(see eqn 2.38) and

$$y = \frac{g_J \mu_B J(B + \lambda M)}{k_B T} \tag{5.7}$$

Reminder: we are assuming $J = S$ and $L = 0$ at this stage.

(see eqn 2.37). Without the λM term due to the molecular field, this would be identical to our treatment of a paramagnet in Section 2.4.3.

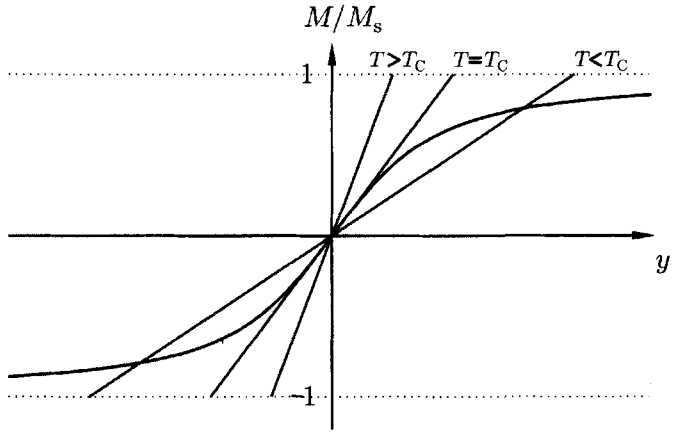

Fig. 5.2 The graphical solution of eqns 5.6 and 5.7 for $B = 0$.

These equations can be solved graphically. First, we restrict our attention to the case of $B = 0$, so that $M = k_B T y / g_J \mu_B J \lambda$. Hence the straight line produced by plotting M against y has a gradient which is proportional to temperature T as illustrated in Fig. 5.2. For high temperature, there is no simultaneous solution of eqns 5.6 and 5.7 except at the origin where $y = 0$ and $M_s = 0$. This situation changes when the gradient of the line is less than that of the Brillouin function at the origin. At low temperatures there are then three solutions, one at $M_s = 0$ and another two for M_s at $\pm$ some non-zero value. It turns out that when the curve is less steep than the Brillouin function at the origin, the non-zero solutions are stable and the zero-solution is unstable. (If the system has $M_s = 0$ for $T < T_C$, any fluctuation, no matter how small, will cause the system to turn into either one of the two stable states.) Thus below a certain temperature, non-zero magnetization occurs and this grows as the material is cooled. The substance thus becomes magnetized, even in the absence of an external field. This **spontaneous magnetization** is the characteristic of ferromagnetism.

The temperature at which the transition occurs can be obtained by finding when the gradients of the line $M = k_B T y / g_J \mu_B J \lambda M_s$ and the curve $M = M_s \mathrm{B}_J(y)$ are equal at the origin. For small y, $\mathrm{B}_J(y) = (J+1)y/3J + O(y^3)$.

The transition temperature, known as the **Curie temperature** T_C, is then defined by

$$T_C = \frac{g_J \mu_B (J+1) \lambda M_s}{3k_B} = \frac{n\lambda\mu_{eff}^2}{3k_B}. \tag{5.8}$$

The molecular field $B_{mf} = \lambda M_s$ is thus $3k_B T_C / g_J \mu_B (J+1)$ and so for a ferromagnet with $J = \frac{1}{2}$ and $T_C \sim 10^3$ K, $B_{mf} = k_B T_C / \mu_B \sim 1500$ T. This is an enormous effective magnetic field and reflects the strength of the exchange interaction.

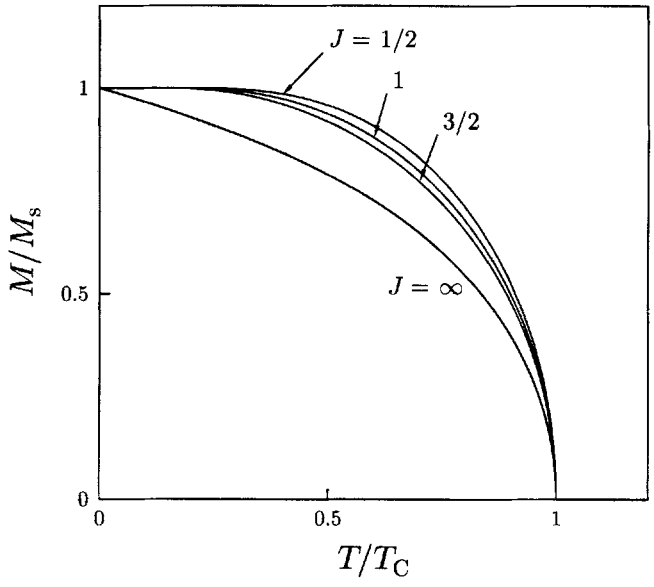

Fig. 5.3 The mean-field magnetization as a function of temperature, deduced for different values of J.

The solutions of these equations as a function of temperature are shown in Fig. 5.3 for a range of values of J. Although the form of the curves is slightly different in each case, some general features persist. The magnetization is zero for temperatures $T \geq T_C$ and is non-zero for $T < T_C$. The magnetization is continuous at $T = T_C$, but its gradient is not. This classifies the phase transition between the non-magnetic and ferromagnetic phases in this molecular field model as a **second-order phase transition**. The order of a phase transition is the order of the lowest differential of the free energy which shows a discontinuity at the transition. A first-order phase transition would have a discontinuous jump in the first derivative of the free energy, i.e. in quantities like the volume, entropy or the magnetization. The jump in the entropy gives a latent heat. A second-order phase transition has a discontinuity in the second derivative of the free energy, i.e. in quantities like the compressibility or the heat capacity. In the present case the discontinuity is in the gradient of the magnetization, i.e. in the second derivative of the free energy, so the transition is second order. Phase transitions and critical exponents will be considered in more detail in Section 6.4. The properties of some common ferromagnets are listed in Table 5.1.

Table 5.1 Properties of some common ferromagnets.

Material	T_C (K)	magnetic moment (μ_B /formula unit)
Fe	1043	2.22
Co	1394	1.715
Ni	631	0.605
Gd	289	7.5
MnSb	587	3.5
EuO	70	6.9
EuS	16.5	6.9

5.1.2 Magnetic susceptibility

Applying a small B field at $T \geq T_C$ will lead to a small magnetization, so that the $y \ll 1$ approximation for the Brillouin function can be used. Thus

$$\frac{M}{M_s} \approx \frac{g_J \mu_B (J+1)}{3k_B} \left(\frac{B + \lambda M}{T} \right) \tag{5.9}$$

so that

$$\frac{M}{M_s} \approx \frac{T_C}{\lambda M_s} \left(\frac{B + \lambda M}{T} \right). \tag{5.10}$$

This can be rearranged to give

$$\frac{M}{M_s} \left(1 - \frac{T_C}{T} \right) \approx \frac{T_C B}{\lambda M_s} \tag{5.11}$$

so that

$$\chi = \lim_{B \to 0} \frac{\mu_0 M}{B} \propto \frac{1}{T - T_C} \tag{5.12}$$

which is known as the Curie Weiss law.

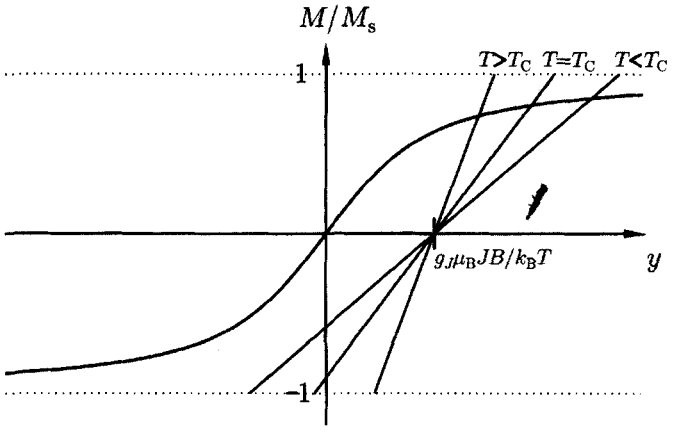

Fig. 5.4 The graphical solution of eqns 5.6 and 5.7 for $B \neq 0$.

5.1.3 The effect of a magnetic field

The effect of adding a magnetic field is to shift to the right the straight line in the graphical solution of the equations (see Fig. 5.4). This results in a solution with $M \neq 0$ for all temperatures and so the phase transition is removed. For ferromagnets in a non-zero magnetic field there is always an energetic advantage to have a non-zero magnetization with the moments lining up along the magnetic field. This removal of the phase transition can be seen in Fig. 5.5 which shows graphical solutions to eqns 5.6 and 5.7 for a range of magnetic fields. In this model it is not necessary to consider the effect of applying a magnetic field in different directions. Whichever direction the magnetic field is applied, the magnetization will rotate round to follow it. The model contains no special direction associated with the ferromagnet itself. In a real ferromagnet this is not the case, and the effect of magnetic anisotropy associated with the material will need to be considered (see the following chapter).

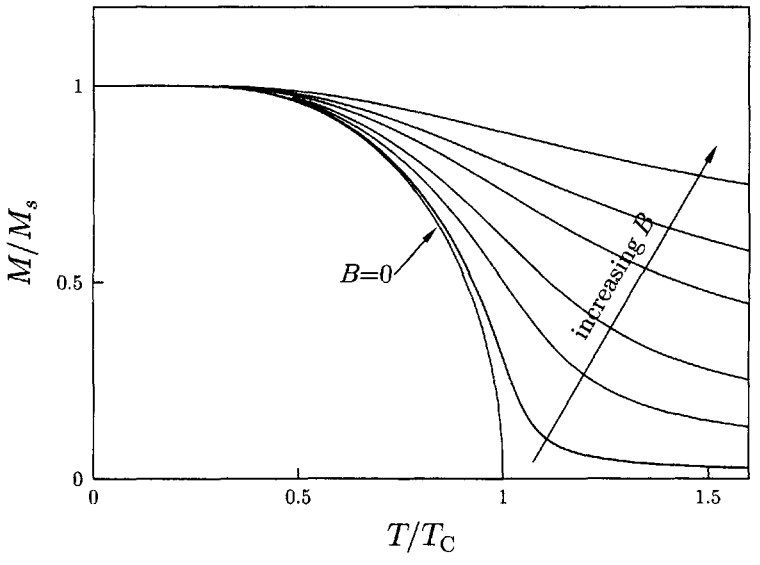

Fig. 5.5 The mean-field magnetization as a function of temperature for $J = \frac{1}{2}$, calculated for different values of the applied field B. The phase transition is only present when $B = 0$.

At $T = T_C$, the effect of the magnetic field is simple to work out analytically. At this temperature, the magnetization is given by $M \propto B^{1/3}$ for small magnetic fields. To prove this, it is necessary to take the next term in the Taylor expansion of $B_J(y)$. Writing $B_J(y) = (J+1)y/3J - \zeta y^3 + O(y^5)$, where ζ is a constant, we must solve simultaneously $M = M_s B_J(y)$ and

$$y = \frac{g_J \mu_B J(B + \lambda M)}{k_B T_C} = \frac{(B + \lambda M)}{\zeta M_s} \tag{5.13}$$

which yields

$$M = M_s \zeta \frac{(B + \lambda M)}{\lambda} - \zeta M_s \left(\frac{3J(B + \lambda M)}{\lambda (J+1) M_s} \right)^3 \tag{5.14}$$

and hence

$$B \propto (B + \lambda M)^3 \tag{5.15}$$

and given that $\lambda M \gg B$, the right-hand side is dominated by the M^3 term so that $M \propto B^{1/3}$.

5.1.4 Origin of the molecular field

When Weiss proposed his molecular field model in 1907 he was disappointed that the constant λ needed to be very large to agree with the large values of T_C found in nature. Considering only dipole fields, it was not possible to account for an internal field which, as discussed above, needs to be $\sim 10^3$ T to account for the Curie temperature of Fe. Thirty years later, Heisenberg showed that it was the exchange interaction, which involves large Coulomb energies, which is responsible for the large molecular field.[4]

The molecular field, parametrized by λ, can be related to the size of the exchange interaction, parametrized by J_{ij}. Assuming that the exchange interaction is effective only over the z nearest neighbours of an ion, where it takes

[4]The molecular field is a convenient fiction and one shouldn't think that magnetic fields $\sim 10^3$ T are experienced by electrons in ferromagnets. The exchange interaction is purely an electrostatic effect. When we talk about the molecular field we are pretending that the exchange interaction is actually internal magnetic field. The point is that, if it really existed and Heisenberg exchange didn't, the molecular field would have to be $\sim 10^3$ T to explain the effects we see.

a value J, then using eqns 5.1, 5.4 and 5.5, one can easily find that

$$\lambda = \frac{2z\mathsf{J}}{ng^2\mu_B^2}. \tag{5.16}$$

Using eqn 5.8, the Curie temperature can then be written

$$T_C = \frac{2z\mathsf{J}J(J+1)}{3k_B}. \tag{5.17}$$

In our discussion so far we have assumed that $L = 0$ and $J = S$. This works for most 3d ions. Exchange is between spin degrees of freedom and therefore depends on S. The magnetic moment of an ion depends on J, the total (spin + orbital) angular momentum. For 3d ions they are the same thing, because L is quenched.

For 4f ions however, **S** is not a good quantum number, but **J** is. It follows that the component of **S** which is perpendicular to **J** must average to zero. The component of **S** which is parallel to **J** is conserved. Thus one must project **S** onto **J**. Now $\mathbf{J} = \mathbf{L} + \mathbf{S}$ and $\mathbf{L} + 2\mathbf{S}$ is equal to $g_J\mathbf{J}$ plus a component perpendicular to **J**. Hence the component of **S** that is a good quantum number is $(g_J - 1)\mathbf{J}$. Values of $(g_J - 1)$ for various 4f ions are listed in Table 5.2. From this, it is clear that **S** and **J** are parallel for the so-called 'heavy rare earths' (Gd to Yb), but antiparallel for the so-called 'light rare earths' (Ce to Sm).

Table 5.2 The g-factors for 4f ions using Hund's rules.

ion	shell	S	L	J	g_J	$g_J - 1$	$(g_J - 1)^2 J(J+1)$
Ce^{3+}	$4f^1$	$\frac{1}{2}$	3	$\frac{5}{2}$	$\frac{6}{7}$	$-\frac{1}{7}$	0.18
Pr^{3+}	$4f^2$	1	5	4	$\frac{4}{5}$	$-\frac{1}{5}$	0.80
Nd^{3+}	$4f^3$	$\frac{3}{2}$	6	$\frac{9}{2}$	$\frac{72}{99}$	$-\frac{27}{99}$	1.84
Pm^{3+}	$4f^4$	2	6	4	$\frac{3}{5}$	$-\frac{2}{5}$	3.20
Sm^{3+}	$4f^5$	$\frac{5}{2}$	5	$\frac{5}{2}$	$\frac{2}{7}$	$-\frac{5}{7}$	4.46
Eu^{3+}	$4f^6$	3	3	0	–	–	–
Gd^{3+}	$4f^7$	$\frac{7}{2}$	0	$\frac{7}{2}$	2	1	15.75
Tb^{3+}	$4f^8$	3	3	6	$\frac{3}{2}$	$\frac{1}{2}$	10.50
Dy^{3+}	$4f^9$	$\frac{5}{2}$	5	$\frac{15}{2}$	$\frac{4}{3}$	$\frac{1}{3}$	7.08
Ho^{3+}	$4f^{10}$	2	6	8	$\frac{5}{4}$	$\frac{1}{4}$	4.50
Er^{3+}	$4f^{11}$	$\frac{3}{2}$	6	$\frac{15}{2}$	$\frac{6}{5}$	$\frac{1}{5}$	2.55
Tm^{3+}	$4f^{12}$	1	5	6	$\frac{7}{6}$	$\frac{1}{6}$	1.17
Yb^{3+}	$4f^{13}$	$\frac{1}{2}$	3	$\frac{7}{2}$	$\frac{8}{7}$	$\frac{1}{7}$	0.32
Lu^{3+}	$4f^{14}$	0	0	0	–	–	–

Using $(g_J - 1)\mathbf{J}$ for the conserved part of **S**, the expression $-\sum_{ij}\mathsf{J}_{ij}\mathbf{S}_i \cdot \mathbf{S}_j$ can be replaced with $-\sum_{ij}(g_J - 1)^2\mathsf{J}_{ij}\mathbf{J}_i \cdot \mathbf{J}_j$. The magnetic moment $\boldsymbol{\mu} = -g_J\mu_B\mathbf{J}$ can then be used to repeat the calculation leading to eqn 5.16, resulting in

$$\lambda = \frac{2z\mathsf{J}(g_J - 1)^2}{ng_J^2\mu_B^2}. \tag{5.18}$$

(For the special case of transition metal ions with orbital quenching, $g_J = 2$ and eqn 5.18 reduces to eqn 5.16.) The Curie temperature can then be written

$$T_C = \frac{2z(g_J - 1)^2 J}{3k_B} J(J+1). \tag{5.19}$$

The critical temperature is therefore expected to be proportional to the **de Gennes factor** $(g_J - 1)^2 J(J+1)$. Values of the de Gennes factor are also listed in Table 5.2. Gd, with the largest de Gennes factor, is a ferromagnet but the rare earth metals show a variety of different ground states, including antiferromagnetism and helimagnetism which will be considered in the next sections.

Pierre-Gilles de Gennes (1932–)

5.2 Antiferromagnetism

If the exchange interaction is negative, $J < 0$, the molecular field is oriented such that it is favourable for nearest neighbour magnetic moments to lie antiparallel to one another. This is **antiferromagnetism**. Very often this occurs in systems which can be considered as two interpenetrating **sublattices** (see Fig. 5.6), on one of which the magnetic moments point up and on the other of which they point down. The nearest neighbours of each magnetic moment in Fig. 5.6 will then be entirely on the other sublattice. Initially we will therefore assume that the molecular field on one sublattice is proportional to the magnetization of the other sublattice. We will also assume that there is no applied magnetic field.

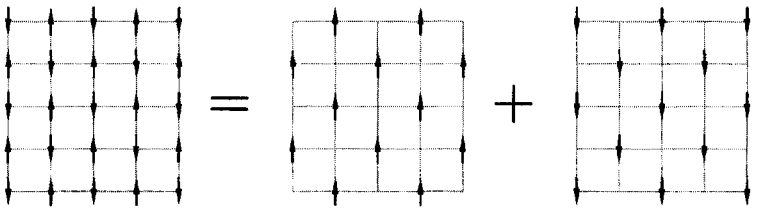

Fig. 5.6 An antiferromagnet can be decomposed into two interpenetrating sublattices.

5.2.1 Weiss model of an antiferromagnet

If we label the 'up' sublattice + and the 'down' sublattice − then the molecular field on each sublattice is

$$\begin{aligned} B_+ &= -|\lambda| M_- \\ B_- &= -|\lambda| M_+, \end{aligned} \tag{5.20}$$

where λ is the molecular field constant which is now negative. On each sublattice, the molecular field is therefore given by

$$M_\pm = M_s B_J\left(-\frac{g_J \mu_B J |\lambda| M_\mp}{k_B T}\right). \tag{5.21}$$

The two sublattices are equivalent in everything except the direction of the moments so that

$$|M_+| = |M_-| \equiv M, \tag{5.22}$$

and hence

$$M = M_s B_J\left(\frac{g_J \mu_B J|\lambda|M}{k_B T}\right). \tag{5.23}$$

This is almost identical to the corresponding equation for ferromagnetism (eqns 5.6 and 5.7), and so the molecular field on each sublattice will follow exactly the form shown in Fig. 5.3 and will disappear for temperatures above a transition temperature, known as the **Néel temperature** T_N, which is then defined by

$$T_N = \frac{g_J \mu_B (J+1)|\lambda| M_s}{3k_B} = \frac{n|\lambda|\mu_{eff}^2}{3k_B}. \tag{5.24}$$

Louis E. F. Néel (1904–2000)

Although the magnetization on each sublattice will follow the form shown in Fig. 5.3, the two magnetizations will be in oppositedirections so that the net magnetization $M_+ + M_-$ of the antiferromagnet will be zero. One can define a quantity known as the **staggered magnetization** as the *difference* of the magnetization on each sublattice, $M_+ - M_-$; this is then non-zero for temperatures below T_N and hence can be used as an order parameter[5] for antiferromagnets.

[5] An order parameter will be defined in Section 6.1.

5.2.2 Magnetic susceptibility

For temperatures above T_N the effect of a small applied magnetic field can be calculated in the same way as for the ferromagnet, by expanding the Brillouin function $B_J(y) = (J+1)y/3J + O(y^3)$, and results in the magnetic susceptibility χ being given by

$$\chi = \lim_{B\to 0} \frac{\mu_0 M}{B} \propto \frac{1}{T + T_N}, \tag{5.25}$$

which is the Curie Weiss law again but with the term $-T_C$ replaced by $+T_N$.

This result gives a ready means of interpreting susceptibility data in the paramagnetic state (i.e. for temperatures above the transition to magnetic order). The magnetic susceptibility can be fitted to a Curie Weiss dependence

$$\chi \propto \frac{1}{T - \theta}, \tag{5.26}$$

where θ is the **Weiss temperature**. If $\theta = 0$, the material is a paramagnet (see eqn 2.44). If $\theta > 0$ the material is a ferromagnet and we expect $\theta = T_C$ (see eqn. 5.12). If $\theta < 0$ the material is a antiferromagnet and we expect $\theta = -T_N$ (see eqn. 5.25). These possibilities are shown in Fig. 5.7.

Experimentally determined Weiss temperatures in antiferromagnets are often a long way from $-T_N$ (see Table 5.3 which contains data for some common antiferromagnets). This discrepancy is largely due to the assumption we have made that the molecular field on one sublattice depends only on the magnetization of the other sublattice. A more realistic calculation is considered in Exercise 5.3.

Applying a magnetic field to an antiferromagnet at temperatures below T_N is more complicated than the case of a ferromagnet below T_C because the *direction* in which the magnetic field is applied is crucial. There is no longer an energetic advantage for the moments to line up along the field because any energy saving on one sublattice will be cancelled by the energy cost for

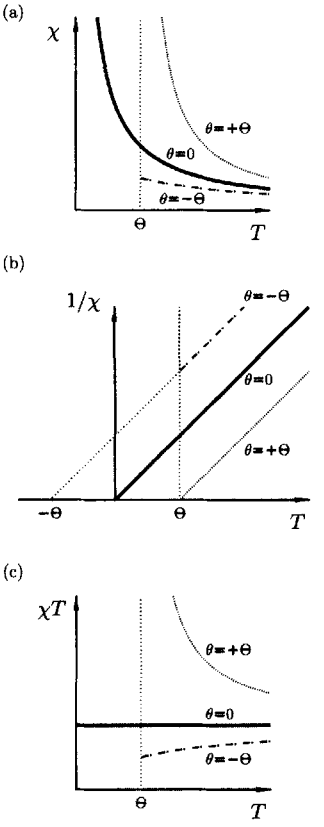

Fig. 5.7 The Curie Weiss law states that $\chi \propto 1/(T-\theta)$ for $T > \theta$. This is shown in (a) for three cases: $\theta = 0$ (paramagnet), $\theta = \Theta > 0$ (ferromagnet) and $\theta = -\Theta < 0$ (antiferromagnet). Straight-line graphs are obtained by plotting $1/\chi$ against T as shown in (b) with the intercept on the temperature axis yielding θ. A graph of χT against T can be constant ($\theta = 0$), increasing for decreasing T ($\theta > 0$) or decreasing for decreasing T ($\theta < 0$), as shown in (c).

Table 5.3 Properties of some common antiferromagnets.

Material	T_N (K)	θ (K)	J
MnF_2	67	−80	$\frac{5}{2}$
MnO	116	−510	$\frac{5}{2}$
CoO	292	−330	$\frac{3}{2}$
FeO	116	−610	2
Cr_2O_3	307	−485	$\frac{3}{2}$
α-Fe_2O_3	950	−2000	$\frac{5}{2}$

the other sublattice, if the magnetization on the two sublattices is equal and opposite.

Consider first the case of absolute zero ($T = 0$), so that thermal agitation effects can be ignored. $|M_+|$ and $|M_-|$ are both equal to M_s. If a small magnetic field is applied *parallel* to the magnetization direction of one of the sublattices (and hence antiparallel to the magnetization direction of the other sublattice), a small term is added or subtracted to the local field of each sublattice. Since both sublattices are already saturated, this has no effect and the net magnetization induced in the material is zero so that $\chi_{\parallel} = 0$. If instead the small magnetic field is applied *perpendicular* to the magnetization direction of one of the sublattices, this causes the magnetization of both sublattices to tilt slightly so that a component of magnetization is produced along the applied magnetic field (see Fig. 5.8). Thus $\chi_{\perp} \neq 0$.

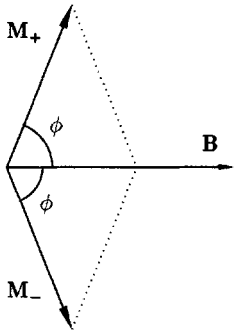

Fig. 5.8 The origin of $\chi_{\perp}$. A small magnetic field B is applied perpendicular to the magnetization direction of the sublattices, causing the magnetization of both sublattices to tilt slightly so that a component of magnetization is produced along the applied magnetic field.

If the temperature is now increased, but still kept below T_N, the thermal fluctuations decrease the molecular field at each sublattice. This greatly affects the case of applying a small magnetic field *parallel* to the magnetization direction of one of the sublattices, since the field enhances the magnetization of one sublattice and reduces it on the other. In the perpendicular case, raising the temperature has little effect since the M_+ and M_- are reduced equally and are also symmetrically affected by the small magnetic field. $\chi_{\perp}$ is independent of temperature, whereas $\chi_{\parallel}$ rises from 0 up to $\chi_{\perp}$ as $T \rightarrow T_N$. These characteristics are shown in Fig. 5.9.

5.2.3 The effect of a strong magnetic field

Let us first consider the effect of a strong magnetic field on an antiferromagnet with $T = 0$ to avoid any complications from thermal fluctuations. If the magnetic field is large enough, it must eventually dominate over any internal molecular field and force all the magnetic moments to lie parallel to each other. But as the field is increased, although the final end result is clear, the route to that destination depends strongly on the direction of the applied field with respect to the initial direction of sublattice magnetization.

If the applied magnetic field is perpendicular to the sublattice magnetizations, all that happens is that as the field increases the magnetic moments bend round more and more (ϕ gets progressively smaller, see Fig. 5.8) until the moments line up with the applied magnetic field.

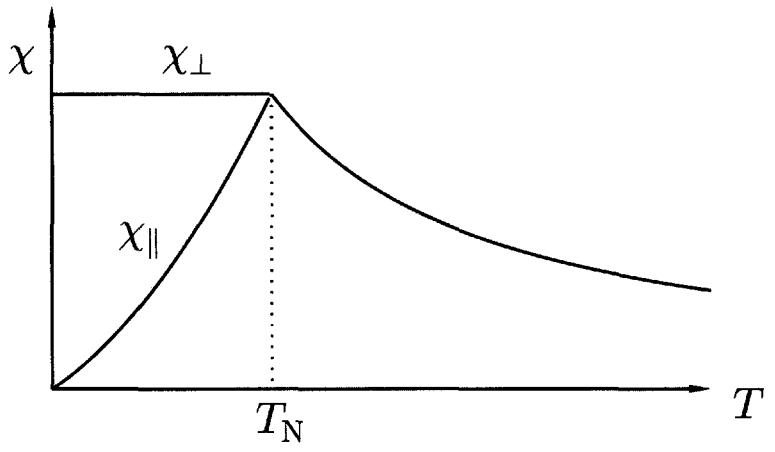

Fig. 5.9 The effect of temperature on $\chi_{\parallel}$ and $\chi_{\perp}$.

If the applied magnetic field is parallel to the sublattice magnetizations, the case is more interesting. At small magnetic fields the moments don't rotate round but stay in line (Fig. 5.10(a)). However, at a critical field the system suddenly snaps into a different configuration (Fig. 5.10(b)); this is called a **spin-flop transition**. For further increases of magnetic field the angle θ gets progressively smaller until eventually the magnetic moments line up with the applied magnetic field.

These effects can be calculated quantitatively. Let $\mathbf{M}_+$ lie at an angle of θ to the magnetic field (measured counterclockwise) and let $\mathbf{M}_-$ lie at an angle of ϕ to the magnetic field (measured clockwise). We will apply the magnetic field along the crystallographic z axis. The antiferromagnetic phase corresponds to $\theta = 0$ and $\phi = \pi$ (see Fig. 5.10(a)) and the spin-flop phase corresponds to $\theta = \phi$. It is necessary to determine which phase has lower energy.

We assume that the total energy E is due to the sum of the Zeeman energies of the individual sublattices and a term representing the exchange coupling which will depend on the relative orientation between the two sublattice moments. This leads to

$$E = -MB\cos\theta - MB\cos\phi + AM^2\cos(\theta + \phi), \tag{5.27}$$

where A is a constant connected with the exchange coupling. To model the magnetic anisotropy, it is necessary to add on a term of the form

$$-\frac{1}{2}\Delta(\cos^2\theta + \cos^2\phi) \tag{5.28}$$

where Δ is a small constant. This accounts for the fact that the magnetizations actually do prefer to lie along a certain crystallographic axis (in this case the z axis) so that that θ and ϕ prefer to be 0 or π but not somewhere in between. In the antiferromagnetic case ($\theta = 0, \phi = \pi$) we have $E = -AM^2 - \Delta$ which is independent of field. In the spin-flop case ($\phi = \theta$) we have

$$E = -2MB\cos\theta + AM^2\cos 2\theta - \Delta\cos^2\theta. \tag{5.29}$$

The condition $\partial E/\partial\theta = 0$ shows that there is a minimum energy when $\theta = \cos^{-1}[B/2AM]$, ignoring the anisotropy term. Substituting this back into E

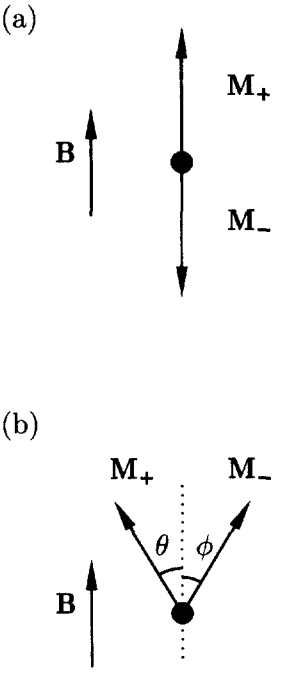

Fig. 5.10 A magnetic field is applied parallel to the sublattice magnetizations. (a) For small fields nothing happens and the system remains in the antiferromagnetic phase. (b) Above a critical field the system undergoes a spin-flop transition into a spin-flop phase.

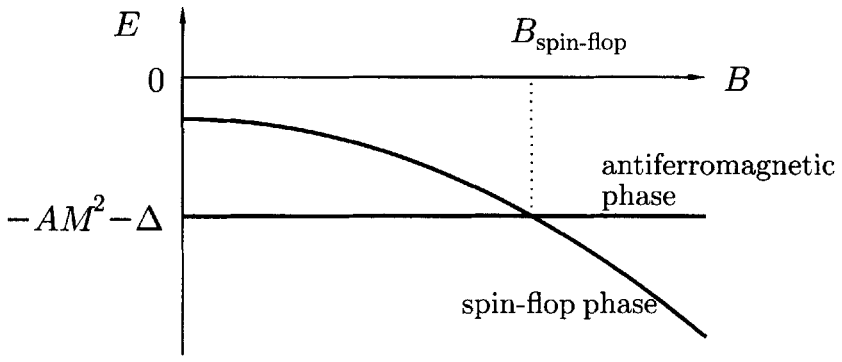

Fig. 5.11 The energy of the antiferromagnetic phase and the spin-flop phase as a function of B.

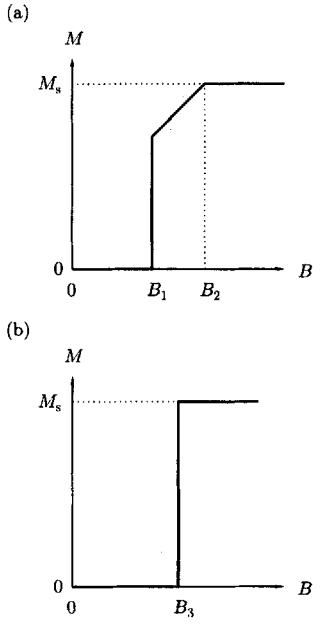

Fig. 5.12 (a) Magnetization for applying a parallel magnetic field to an antiferromagnet. Initially nothing happens but then there is a spin-flop transition to a spin-flop phase at B_1. The magnetic field then rotates the moments until saturation is achieved at the field B_2. (b) If there is a strong preference for the spins to lie along the parallel direction, no spin-flop occurs. Instead there is a spin-*flip* transition at B_3. Both figures show the expected curves for absolute zero. Finite temperature will round off the sharp corners. This is also known as a metamagnetic transition.

and plotting the result leads to the graph shown in Fig. 5.11. Below the critical field $B_{\text{spin-flop}}$ the antiferromagnetic case has the lowest energy. At the critical field $B_{\text{spin-flop}}$ the system switches from one state to the other and we have a spin-flop transition. Above this field the spin-flop phase has the lowest energy.

The magnetization for the antiferromagnet in a large parallel magnetic field is shown in Fig. 5.12(a). There is no effect until the spin-flop transition, above which the magnetization increases steadily until saturation is reached. If the anisotropy effect is very strong (Δ is large), another effect can occur. In this case, if the external field is along z, no spin-flop occurs. Instead we get a spin-flip transition, i.e. the magnetization of one sublattice suddenly reverses when B reaches a critical value, and the system moves in a single step to the ferromagnetic state. This is illustrated in Fig. 5.12(b).

5.2.4 Types of antiferromagnetic order

Another complication with antiferromagnetism is that there is a large number of ways of arranging an equal number of up and down spins on a lattice. The different possible arrangements also depend on the kind of crystal lattice on which the spins are to be arranged. A selection of possible arrangements is shown in Figures 5.13 and 5.14.

In cubic perovskites, which have the magnetic atoms arranged on a simple cubic lattice, G-type ordering (see Fig. 5.13(d)) is very common because superexchange interactions through oxygen atoms force all nearest-neighbour magnetic atoms to be antiferromagnetically aligned. This is the case for G-type ordering only and is, for example, found in $LaFeO_3$ and $LaCrO_3$. $LaMnO_3$ is also a cubic perovskite but shows A-type ordering (see Fig. 5.13(a)), with alternately aligned ferromagnetic (100) planes. This occurs because of the Jahn–Teller distortion of the Mn^{3+} ions which gives alternate long and short Mn–O bonds within the (100) planes. The orbitals on adjacent Mn^{3+} ions are differently oriented, and the superexchange leads to an interaction between an occupied orbital on one atom with an unoccupied orbital on its neighbour. The in-plane interaction is thus ferromagnetic while the out-of-plane interaction is antiferromagnetic because of the conventional operation of the superexchange interaction.

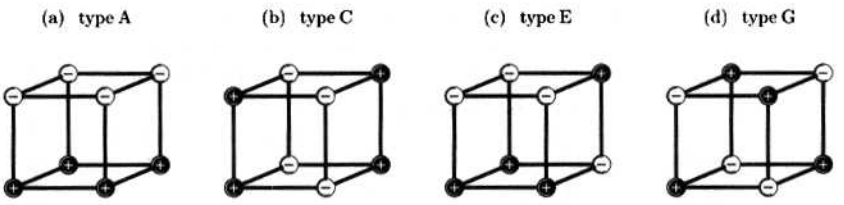

Fig. 5.13 Four types of antiferromagnetic order which can occur on simple cubic lattices. The two possible spin states are marked + and −.

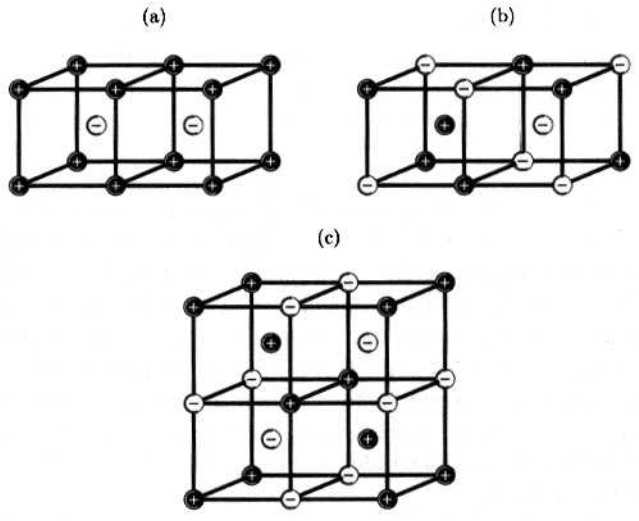

Fig. 5.14 Three types of antiferromagnetic order which can occur on body-centred cubic lattices.

5.3 Ferrimagnetism

The above treatment of antiferromagnetism assumed that the two sublattices were equivalent. But what if there is some crystallographic reason for them not to be equivalent? In this case the magnetization of the two sublattices may not be equal and opposite and therefore will not cancel out. The material will then have a net magnetization. This phenomenon is known as **ferrimagnetism**. Because the molecular field on each sublattice is different, the spontaneous magnetizations of the sublattices will in general have quite different temperature dependences. The net magnetization itself can therefore have a complicated temperature dependence. Sometimes one sublattice can dominate the magnetization at low temperature but another dominates at higher temperature; in this case the net magnetization can be reduced to zero and change sign at a temperature known as the **compensation temperature**. The magnetic susceptibilities of ferrimagnets therefore do not follow the Curie Weiss law.

Ferrites are a family of ferrimagnets. They are a group of compounds with the chemical formula $MO{\cdot}Fe_2O_3$ where M is a divalent cation such as Zn^{2+}, Co^{2+}, Fe^{2+}, Ni^{2+}, Cu^{2+} or Mn^{2+}. The crystal structure is the **spinel** structure which contains two types of lattice sites, tetrahedral sites (with four oxygen

Table 5.4 Properties of some common ferrimagnets.

Material	T_C (K)	magnetic moment (μ_B/formula unit)	Compensation temperature (K)
Fe_3O_4	858	4.1	–
$CoFe_2O_4$	793	3.7	–
$NiFe_2O_4$	858	2.3	–
$CuFe_2O_4$	728	1.3	–
$Y_3Fe_5O_{12}$	560	5.0	–
$Gd_3Fe_5O_{12}$	564	16.0	290
$Dy_3Fe_5O_{12}$	563	18.2	220
$Ho_3Fe_5O_{12}$	567	15.2	137

neighbours, these are known as A sites) and octahedral sites (with six oxygen neighbours, these are known as B sites). There are twice as many B sites as A sites. The two sublattices are non-equivalent because there are two types of crystallographic site and they contain two types of different ion. In **normal spinels**, the M^{2+} cations sit at the A sites and the Fe^{3+} ($^6S_{5/2}$ and therefore a moment of 5 μ_B) cations sit at the B sites. In **inverse spinels** the M^{2+} cations sit at half of the B sites, while the Fe^{3+} cations occupy the other half of the B sites and all the A sites. In inverse spinels, the moments of the Fe^{3+} cations on the A and the B sites are antiparallel, so that the total moment of the sample is due to the M^{2+} ions only.

The case of M=Fe, i.e. Fe_3O_4 (which is a semiconductor, in contrast to the other ferrites which are insulators), has already been discussed in Section 4.2.5.

Another family of ferrimagnets is the **garnets** which have the chemical formula $R_3Fe_5O_{12}$ where R is a trivalent rare earth atom. The crystal structure is cubic, but the unit cell is quite complex. Three of the Fe^{3+} ions are on tetrahedral sites, two are on octahedral sites and the R^{3+} ions are on sites of dodecahedral symmetry. In yttrium iron garnet (YIG), $Y_3Fe_5O_{12}$, the Y^{3+} has no magnetic moment (it is $4d^0$) and the moments of the Fe^{3+} ions on the tetrahedral sites are antiparallel to those on the octahedral sites, so that the net moment is $5\mu_B$.

Barium ferrite ($BaFe_{12}O_{19} = BaO{\cdot}6Fe_2O_3$) has a hexagonal structure. Eight of the Fe^{3+} ions are antiparallel to the other four, so that the net moment is equivalent to four Fe^{3+} ions, i.e. $20\mu_B$. In powder form, it is used in magnetic recording since it has a high coercivity (see Section 6.7.9). The properties of some common ferrimagnets are listed in Table 5.4.

Most ferrimagnets are electrical insulators and this fact is responsible for many of their practical applications. Ferromagnets are often metallic and thus are unsuitable in applications in which an oscillating magnetic field is involved; a rapidly changing magnetic field induces a voltage and causes currents (known as eddy currents) to flow in conductors. These currents cause resistive heating in a metal (eddy current losses). Many ferrimagnets therefore can be used when a material with a spontaneous magnetization is required to operate at high frequencies, since the induced voltage will not be able to cause any significant eddy currents to flow in an insulator. Solid ferrite cores are used in

many high frequency applications including aerials and transformers requiring high permeability and low energy loss, as well as applications in microwave components. Also many ferrimagnets are more corrosion resistant than metallic ferromagnets since they are already oxides.

5.4 Helical order

In many rare earth metals, the crystal structure is such that the atoms lie in layers. Consider first the case (relevant for dysprosium) in which there is ferromagnetic alignment of atomic moments within the layers and that the interaction between the layers can be described by a nearest-neighbour exchange constant J_1 and a next-nearest-neighbour exchange constant J_2. If the angle between the magnetic moments in successive basal planes (i.e. the planes corresponding to the layers) is θ (see Fig. 5.15(a)), then the energy of the system can be written

$$E = -2NS^2(J_1 \cos\theta + J_2 \cos 2\theta), \tag{5.30}$$

where N is the number of atoms in each plane. The energy is minimized when $\partial E/\partial\theta = 0$ which yields

$$(J_1 + 4J_2 \cos\theta)\sin\theta = 0. \tag{5.31}$$

Solutions to this are either $\sin\theta = 0$, which implies $\theta = 0$ or $\theta = \pi$ (ferromagnetism or antiferromagnetism), or

$$\cos\theta = -\frac{J_1}{4J_2}. \tag{5.32}$$

This last solution corresponds to helical order (also known as **helimagnetism**) and is favoured over either ferromagnetism or antiferromagnetism when $J_2 < 0$ and $|J_1| < 4|J_2|$ (see Fig. 5.15(b)). The pitch of the spiral will not in general be commensurate with the lattice parameter and so no two layers in a crystal will have exactly the same spin directions.

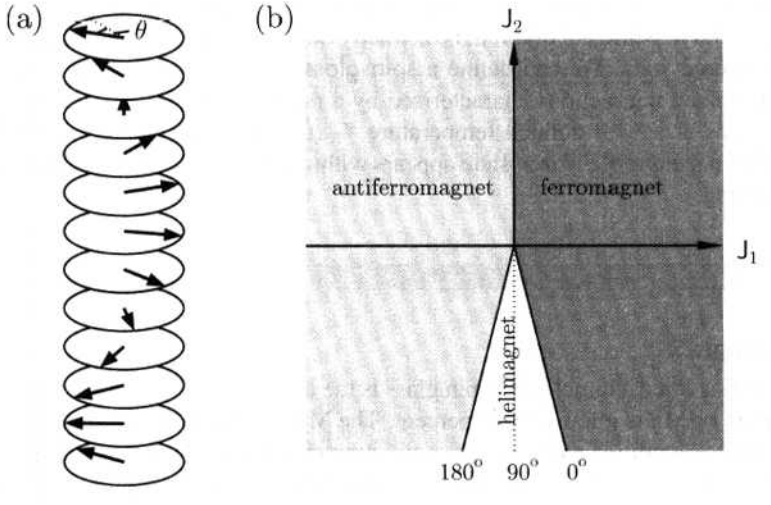

Fig. 5.15 (a) Helimagnetic ordering. (b) The phase diagram for the model of planes coupled by a nearest-neighbour exchange constant J_1 and a next-nearest-neighbour exchange constant J_2.

Helical structures are found in many magnetic systems, most famously in rare earth metals. Many of these rare earth metals have hexagonally close packed crystal structures. The axis of the helix is perpendicular to the hexagonally close packed planes, along what is usually defined as the c axis. The plane in which the spins rotate in Tb, Dy and Ho is the hexagonally close packed plane, but in Er and Tm the easy axis for spins is the c axis so that the c component of the spins is modulated sinusoidally over a certain temperature range. Spiral structures (Fig. 5.1(d)) are also possible in which the spins have a component along the easy axis, perpendicular to the plane, but also a component in the plane which precesses around a helix.

The exchange interaction in rare earth metals is an indirect RKKY interaction mediated by the conduction electrons. It has much longer range than superexchange interactions and changes its sign as a function of distance. The model presented above, which contains just nearest and next-nearest neighbour interactions, is therefore an over-simplification. Details of the Fermi surface of each rare earth metal are needed to compute the wave vector-dependent exchange interaction $J(\mathbf{q})$. If this takes a maximum at a certain wave vector $\mathbf{q}$, then helimagnetism can be induced with wave vector $\mathbf{q}$. A further feature is the large effect of the crystal field in rare earth metals. The crystal field splits the electronic states and usually one finds that not only the ground state but also some excited states of the system are thermally populated, further complicating the analysis that needs to be performed to understand these systems.

5.5 Spin glasses

So far we have considered materials in which there is one or more magnetic moments in each unit cell. What happens if we start with a non-magnetic lattice and sparsely populate it with a dilute, random distribution of magnetic atoms? One's intuition might suggest that the end result would be something which is entirely random which would not be likely to exhibit a phase transition from a high temperature disordered state to a low temperature ordered state. This is only partly right because such systems, although inherently random, do show something approximating to a phase transition at a particular temperature to a state which, while not ordered, is distinctly different from the high temperature disordered state. We can define a **spin glass** as a random, magnetic system with mixed interactions characterized by a random, yet cooperative, freezing of spins at a well defined temperature T_f (the freezing temperature) below which a metastable frozen state appears without the usual magnetic long-range ordering.

Example 5.1

A well studied example of a spin glass is the alloy CuMn in which the concentration of Mn is a few atomic percent. The Mn ions are therefore present only in dilute quantities and their magnetic moments interact with each other via a RKKY (see sections 4.2.4 and 7.7.3) interaction mediated by the conduction